JOC The Journal of Organic Chemistry

Article

pubs.acs.org/joc

meta versus *para* Substitution: How Does C−H Activation in a Methyl Group Occur in 3-Methylbenzophenone but Does Not Take Place in 4-Methylbenzophenone?

Jiani Ma, Tao Su, Ming-De Li, Xiting Zhang, Jinqing Huang, and David Lee Phillips*

Department of Chemistry, The University of Hong Kong, Pokfulam Road, Hong Kong SAR, People's Republic of China

Supporting Information

ABSTRACT: The photophysical and photochemical reactions of 3-methylbenzophenone (3-MeBP) and 4-methylbenzophenone (4-MeBP) were investigated using femtosecond transient absorption (fs-TA) and nanosecond time-resolved resonance Raman (ns-TR^3) spectroscopy and density functional theory (DFT) calculations. 3-MeBP and 4-MeBP were observed to behave similarly to their parent compound benzophenone (BP) in acetonitrile and isopropyl alcohol solvents. However, in acidic aqueous solutions, an unusual acid-catalyzed proton exchange reaction (denoted the *m*-methyl activation) of 3-MeBP (with a maximum efficiency at pH 0) is detected to compete with a photohydration reaction. In contrast, only the photohydration reaction was observed for 4-MeBP under the acidic pH conditions investigated. How the *m*-methyl activation takes place after photolysis of 3-MeBP in acid aqueous solutions is briefly discussed and compared to related photochemistry of other *meta*-substituted aromatic carbonyl compounds.

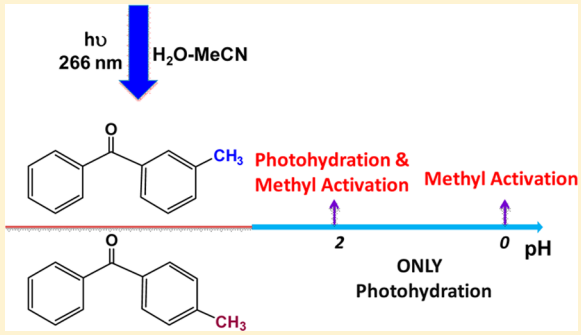

INTRODUCTION

The protonation of the carbonyl oxygen in the excited state of aromatic carbonyl compounds in acid aqueous solutions has been of interest from a variety of perspectives in photochemistry.[1,2] For instance, the protonation of the carbonyl oxygen in the excited states of benzophenone (BP) and acetophenone (AP) was observed to be involved in the photohydration reactions that take place in acid aqueous solutions by Wirz and co-workers.[1] The protonated triplet BP (^{3}BPH$^+$) species was observed to be the key reactive intermediate that underwent hydration of the phenyl ring mainly at the *meta* position accompanied by a minor amount at the *ortho* position.[1] The acid-catalyzed photohydration reaction of BP was found to be reversible, while the *meta*-substituted fluorinated BP derivative was found to undergo an intriguing aromatic photosubstitution reaction to efficiently produce the corresponding *m*-hydroxy-substituted BP derivative.[1] In addition, protonation of the carbonyl oxygen of the aromatic carbonyl group was also thought to be involved in unusual photoredox reactions that occur in acidic aqueous solutions for BP and anthraquinone (AQ) compounds containing a hydroxymethyl group at a *meta* position.[2] These earlier studies by Wan and co-workers[2] revealed that the ketone is reduced to an alcohol and the side chain alcohol is oxidized to its ketone form.[2] In contrast, no photoredox reactions were observed for the analogous *para*-substituted BP and AQ compounds.[2] Therefore, these photoredox reactions were tentatively thought to arise from some sort of "*meta* effect".[2,3] Due to the limitations of traditional steady-state measurements, the photoredox reaction mechanism remained unclear at that time. To gain further information on the reactive intermediates involved in the unusual photoredox reactions, we previously carried out a time-resolved spectroscopic study on 3-(hydroxymethyl)benzophonone (*m*-BPOH) as an example of the molecular system.[4] This work directly probed the reactive intermediates and demonstrated that a key biradical intermediate was involved in the unusual photoredox reaction.[4] Next, we investigated how and when photoredox reactions take place for related AQ compounds, taking 2-(1-hydroxyethyl)-9,10-anthraquinone (2-HEAQ) as a representative molecular system.[5] These studies determined that the photoredox reactions proceed via an initial protonation on the carbonyl oxygen, followed by deprotonation of the methylene C−H bond for both the *m*-BPOH and 2-HEAQ molecules.[4,5] The overall photoredox reaction appears to take place by an enhanced activation of the "distal" *meta* methyl group, which may be thought of as a *m*-methyl activation.

There is also evidence that *m*-methyl activation takes place after photolysis of 3-methylacetophenone and 3-methylbenzophenone (3-MeBP) in acidic aqueous solutions (see the proposed reaction mechanism in Scheme 1) on the basis of results from mass spectroscopy, ^{1}H NMR spectra, and deuterium-substituted product analysis.[2] For example, photolysis of 3-MeBP in acidic D_2O (CH_3CN cosolvent) (pD <3) resulted in efficient introduction of deuterium to the *m*-methyl moiety, implying the C−H bond in the *m*-methyl group was cleaved and a C−D bond formed with the D_2O solvent as the

Received: February 28, 2013
Published: April 15, 2013

Scheme 1. Proposed Reaction Mechanism of *meta* Methyl Activation for 3-MeBP by Wan and Co-Workers[2c]

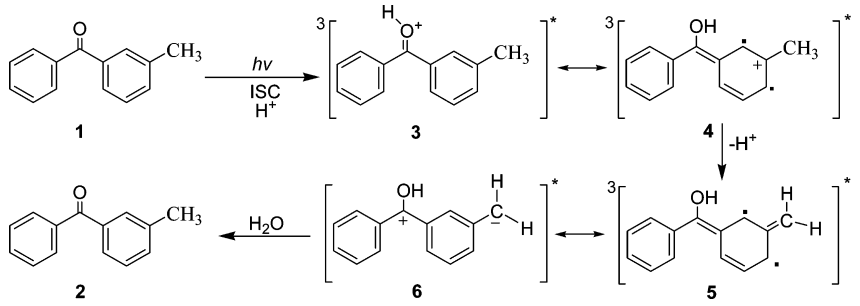

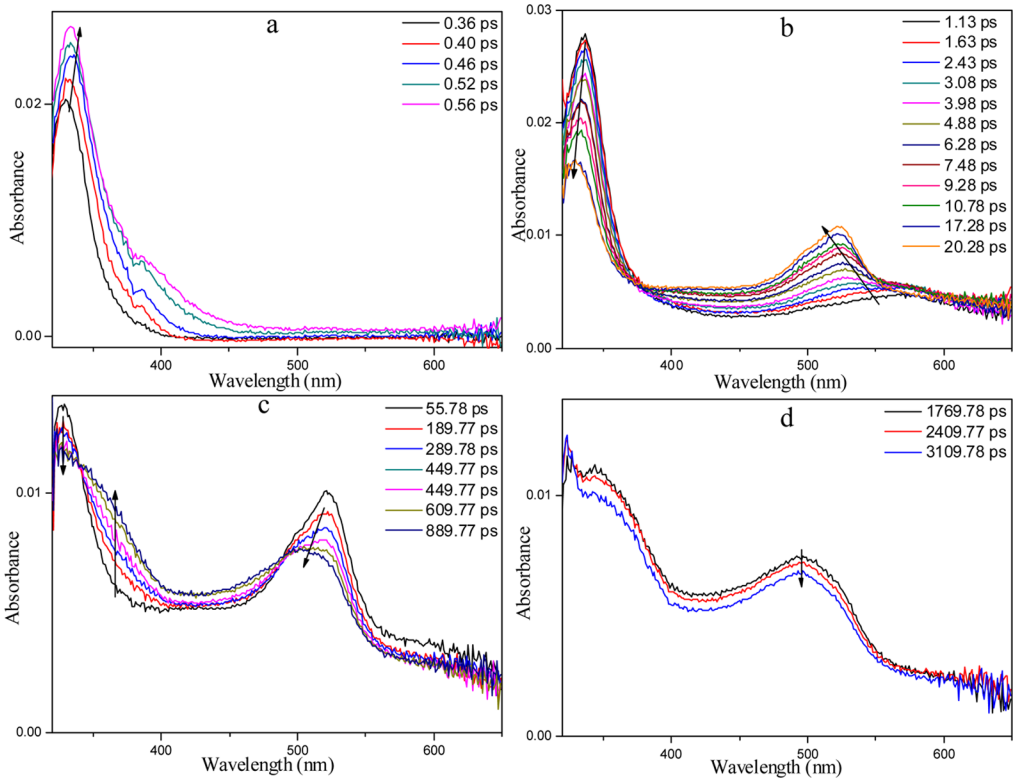

Figure 1. fs-TA spectra of 3-MeBP in a pH 1 CH_3CN/H_2O (1/1) solution observed after 267 nm excitation.

source of the D atom(s).[2] The photolysis of the *p*-methyl-substituted BP (4-MeBP) under analogous conditions gave no reaction. Photolysis of 3-MeBP in neutral D_2O solution or a deuterated organic solvent such as CD_3CN also did not produce any deuterium incorporation reaction product. Therefore, the unusual deuterium incorporation in the *m*-methyl group observed after photolysis of 3-MeBP in acid–D_2O aqueous solutions appears to be associated with some *meta* effect and also an acid-catalyzed process similar to those seen for the photohydration reactions of BP, the photosubstitution reactions of the *m*-fluorine-substituted BP and the photoredox reactions of the *m*-hydroxymethyl-substituted BP and AQ derivatives.[1−5] Although useful information and data have been acquired from previous steady-state and time-resolved studies, the interpretation of the apparent *m*-methyl activation is somewhat ambiguous and not straightforward due to coexisting intermediates from competing photoreduction and photohydration reactions. So far, there have been relatively few direct comparative studies on *meta*- and *para*-substituted aromatic carbonyl compounds in acidic aqueous solutions using time-resolved spectroscopy techniques. In order to obtain a better understanding of the *m*-methyl activation reactions of 3-MeBP in acidic aqueous solutions, we report here a systematic study using femtosecond transient absorption (fs-TA) and nanosecond time-resolved resonance Raman (ns-TR[3]) spectroscopic experiments and density functional theory (DFT) calculations on 3-MeBP and 4-methylbenzophenone (4-MeBP) in acidic aqueous solutions. These experiments directly detect the electronic excited states and intermediates associated with the photophysics and photochemistry of 3-MeBP and 4-MeBP in various solutions, including acidic aqueous solutions. This new information is used to elucidate how the *m*-methyl activation in 3-MeBP takes place and can account for the product analysis observation by Wan and co-workers that photolysis of 3-MeBP in acidic D_2O (CH_3CN cosolvent) (pD <3) led to an efficient introduction of deuterium to the *m*-methyl moiety.[2] These new data also help explain why there is no apparent analogous methyl activation seen at the *para* position in 4-MeBP for photolysis done under corresponding conditions.[2] We compare and contrast the reactivity of the key intermediates and their reaction mechanisms for the *m*-methyl activation of 3-MeBP observed here to those recently observed for the photoredox

dx.doi.org/10.1021/jo400413t | J. Org. Chem. 2013, 78, 4867−4878

reaction of *m*-BPOH. We also briefly discuss these *m*-methyl activation processes in relation to the photohydration reactions of BP and the photosubstitution reactions of the *m*-fluorine-substituted BP derivatives.

RESULTS AND DISCUSSION

A. fs-TA and ns-TR^3 Experimental Study. Time-resolved spectroscopic studies of 3-MeBP and 4-MeBP in an inert organic solvent such as CH_3CN and a strong hydrogen donor solvent such as isopropyl alcohol (IPA) are important for understanding their photophysics and photoreduction reactions and will also serve as benchmarks for comparison to spectra obtained in aqueous solutions where the unusual *m*-methyl activation reactions for 3-MeBP appear to occur. The fs-TA and ns-TR^3 experimental results and discussion for 3-MeBP and 4-MeBP in CH_3CN and IPA are presented in the Supporting Information (see Figures 2S−10S). Both 3-MeBP and 4-MeBP undergo an efficient intersystem crossing (ISC) process from their singlet excited state (S_1) to their triplet excited state in CH_3CN. The triplet excited state of 3-MeBP (denoted as ^{3}(3-MeBP) hereafter) has Raman bands at 938, 970, 1170, 1230, 1374, and 1545 cm^{-1} in its ns-TR^3 spectra. In IPA, the triplet excited state species experiences a photoreduction reaction that produces a ketyl radical intermediate. The photophysics and photochemical reactions of 3-MeBP and 4-MeBP in CH_3CN and IPA resemble those of their parent compound BP (see Figure 11S, Supporting Information). This indicates that the methyl group substituent at the *meta* or *para* position does not exert much influence on the photophysical and photoreduction reactions of the BP derivative in nonaqueous solutions.

Figure 1 displays the fs-TA results for 3-MeBP in a pH 1 CH_3CN/H_2O (1/1) solution. Similar to the fs-TA results obtained in a CH_3CN solution (Figure 2S, Supporting Information), the red-shifted spectral profile shown in Figure 1a is due to the internal conversion (IC) process from a higher excited state (S_n ($n > 1$)) to the lowest singlet excited state (S_1). Thereafter, an intersystem crossing (ISC) process is observed and the ^{3}(3-MeBP) species absorbs at 326 and 522 nm (Figure 1b). The isosbestic point in the fs-TA spectra of 3-MeBP blue-shifts from 385 nm in CH_3CN to 378 nm in the CH_3CN/H_2O (1/1) pH 1 solution, and this is likely due to hydrogen-bonding effects that occur in the aqueous solution. The observation of clear isosbestic points at 339 and 490 nm (Figure 1c) indicates that ^{3}(3-MeBP) forms a new species that has a broad band from 330 to 400 nm and another band around 500 nm.

As the delay time increased, the newly formed species decayed without any other species produced (Figure 1d). Because it has been well documented that aromatic ketones become more basic in their excited state in comparison to their ground state,[1] the new species is probably the triplet protonated species of 3-MeBP at the carbonyl oxygen, which is denoted as ^{3}(3-MeBP·H$^+$), and this is the intermediate **3** shown in Scheme 1. TD-DFT calculations were performed for ^{3}(3-MeBP·H$^+$) in the presence of water. The simulated absorption spectrum (Figure 2) using GaussSum software[6] exhibited good agreement with the experimental spectra recorded at later delay times in a pH 1 CH_3CN/H_2O (1/1) solution, and this provides further support for the assignment of the new species as ^{3}(3-MeBP·H$^+$). Detection of ^{3}(3-MeBP·H$^+$) corroborates that protonation of the carbonyl oxygen in the BP group is the reason for the decay of ^{3}(3-MeBP), and this is similar to analogous reactions observed in studies on BP, *m*-BPOH, and 2-HEAQ in acidic aqueous solutions.[1b,4,5] The pK_a for the triplet protonated excited state BP was determined to be −0.4 ± 0.1 by Wirz and co-workers,[1b] and it may be reasonable to estimate a similar value for ^{3}(3-MeBP·H$^+$).

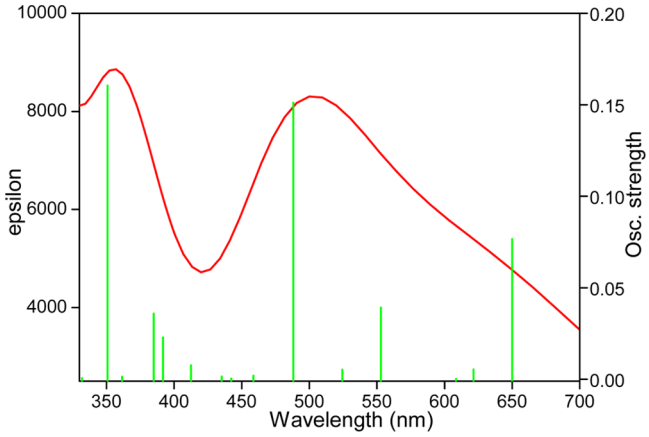

Figure 2. Simulated absorption spectra of ^{3}(3-MeBP·H$^+$) obtained from TD-DFT calculations employing BPW91/cc-PVDZ in the presence of H_2O. The theoretical curve was obtained using the program GaussSum 2.2 with fwhm = 5000 cm^{-1}. The excited states are shown as vertical lines with their height equal to the computed extinction coefficient.

The temporal dependence of the transient absorption at 525 nm for 3-MeBP was inspected in mixed aqueous solutions with varying pH values and can be fitted simultaneously by a two-exponential function (Figure 3 and Table 1). In a pH 1

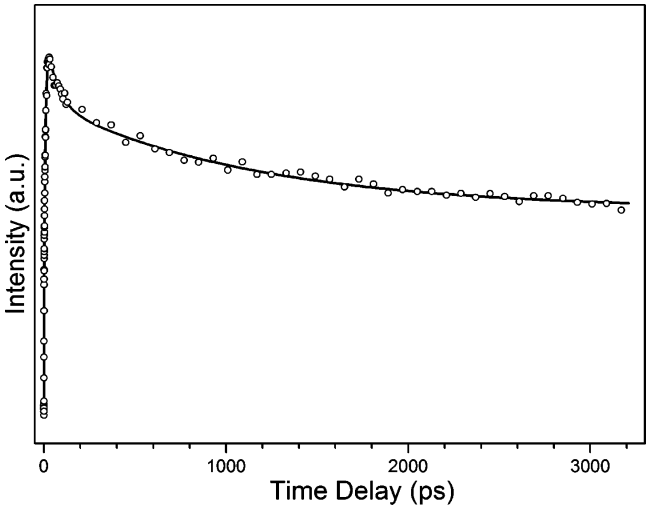

Figure 3. Temporal dependence of the transient absorption at 525 nm for 3-MeBP in a pH 1 CH_3CN/H_2O (1/1) solution. The solid line indicates a kinetics fitting to the experimental data points using a two-exponential function.

Table 1. Time Constants for the Temporal Dependence of the Absorbance at 525 nm from the fs-TA Experiments of 3-MeBP in CH_3CN/H_2O (1/1) Solutions with Different pH Values

	pH 2	pH 1
τ_1 (ps)	6.9 ± 0.1	6.2 ± 0.2
τ_2 (ps)	1343 ± 30	1294 ± 30

dx.doi.org/10.1021/jo400413t | J. Org. Chem. 2013, 78, 4867−4878

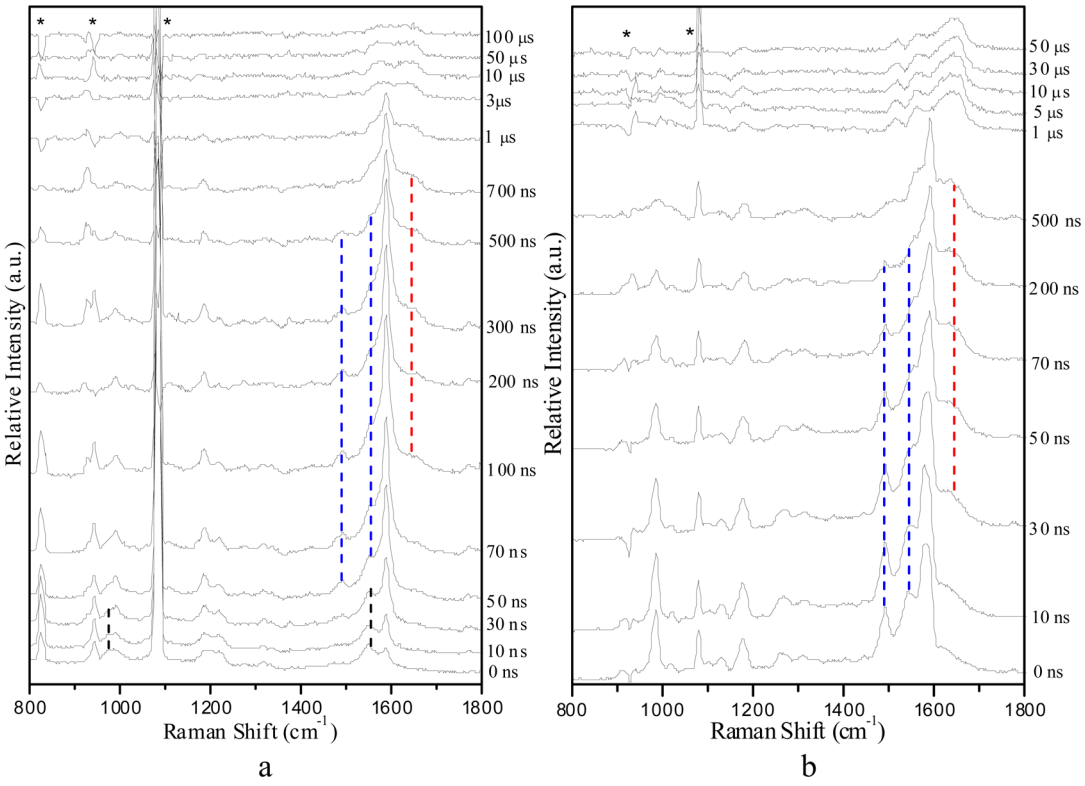

Figure 4. ns-TR^3 spectra of 2.0×10^{-3} M 4-MeBP in CH_3CN/H_2O (1/1) solutions with (a) pH 2 and (b) pH 0 obtained after 266 nm excitation with a probe wavelength of 319.9 nm.

solution, the time constant value of 6.2 ps is attributed to the lifetime of the ^{3}(3-MeBP) intermediate, which is shorter than that in CH_3CN (see the Supporting Information for more details), and this suggests that ^{3}(3-MeBP) is the reactive precursor to the photochemistry events that subsequently occur in aqueous solutions. The other time constant of 1294 ps is assigned to the lifetime of ^{3}(3-MeBP·H$^+$). The shorter lifetimes of ^{3}(3-MeBP) and ^{3}(3-MeBP·H$^+$) in a stronger acid solution suggest that the photochemical reaction for 3-MeBP in an aqueous solution is facilitated by acid. Similar fs-TA results were obtained for 4-MeBP in acidic aqueous solutions (see Figure 10S, Supporting Information), and these results also suggested that ^{3}(4-MeBP·H$^+$) was produced from protonation of ^{3}(4-MeBP). After directly probing ^{3}(3-MeBP·H$^+$) and ^{3}(4-MeBP·H$^+$) in acidic aqueous solutions by fs-TA, ns-TR^3 experiments were done in aqueous solutions with different pH values to examine events on the nanosecond time scale and also provide direct structural information for the reactive intermediate species observed. To simplify the discussion, the photochemical reactions of 4-MeBP are detailed first.

Figure 4a displays ns-TR^3 spectra of 4-MeBP measured in a pH 2 CH_3CN/H_2O (1/1) solution. The first species observed (marked with a black dashed line) is assigned to be ^{3}(4-MeBP), from a comparison to ns-TR^3 spectra obtained in CH_3CN (see Figure 7S, Supporting Information). As ^{3}(4-MeBP) is quenched, a new species (marked with blue dashed lines) is generated with a specific Raman band at 1492 cm^{-1}. At later times, a third species (marked with a red dashed line) is seen with a representative band at 1653 cm^{-1}. Under a more strongly acidic aqueous solution (pH 0, Figure 4b), the Raman signals of ^{3}(4-MeBP) are not detected, while the intensity of the Raman bands at 1492 and 1653 cm^{-1} are remarkably enhanced. These results indicate that the two new species are produced from ^{3}(4-MeBP) and are likely related to an acid-catalyzed reaction. On the one hand, the strikingly different spectra profile of Figure 4 in comparison to that obtained in IPA (Figure 9S, Supporting Information) suggests that photoreduction is not the reaction that takes place in acidic aqueous solutions. The great similarity of the behaviors of 4-MeBP in CH_3CN and IPA solvents with its parent compound BP reminds us that the main reaction detected for 4-MeBP in acidic aqueous solutions is probably the photohydration reaction that has also been observed for BP in acid aqueous solutions.[1b,7]

Time-resolved studies on BP have revealed that the triplet state of the hydration species at a *meta* position (denoted as *m*-^{3}(BP·H_2O)) and the singlet state of the hydration species at an *ortho* position (denoted as *o*-^{1}(BP·H_2O)) are the two main intermediates observed during the photohydration reaction of BP in acidic aqueous solutions.[1b,11] The *o*-^{1}(BP·H_2O) species has a long lifetime of several minutes.[1b,7] Similarly, the early (marked with a blue dashed line) and late (marked with a red dashed line) species observed after decay of ^{3}(4-MeBP) in Figure 4 are tentatively assigned as the triplet state of *meta* hydration and the singlet state of *ortho* hydration species of 4-MeBP, and these are denoted as *m*-^{3}(4-MeBP·H_2O) and *o*-^{1}(4-MeBP·H_2O), respectively. This assignment gains support from two aspects. First, the experimental Raman spectra of the two species are quite similar to those of *m*-^{3}(BP·H_2O) and *o*-^{1}(BP·H_2O),[11] respectively. Second, the experimental Raman spectra exhibit good agreement with the vibrational frequency patterns of the respective calculated Raman spectra of *m*-^{3}(4-MeBP·H_2O) (Figure 5) and *o*-^{1}(4-MeBP·H_2O) (Figure 12S, Supporting Information). When the fs-TA and ns-TR^3 results are combined, it can be concluded that 4-MeBP undergoes an ISC process to form ^{3}(4-MeBP) that is then protonated at the

dx.doi.org/10.1021/jo400413t | J. Org. Chem. 2013, 78, 4867−4878

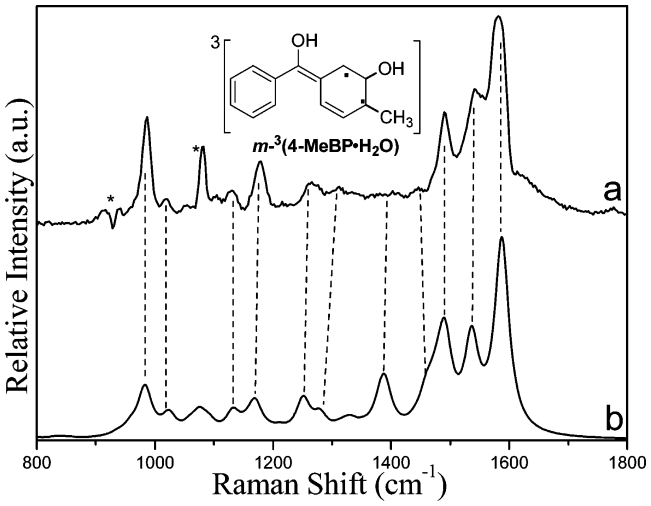

Figure 5. Comparison of (a) the experimental Raman spectrum obtained at 0 ns time delay in a pH 0 CH_3CN/H_2O (1/1) solution with 2.0×10^{-3} M 4-MeBP to (b) the calculated normal Raman spectrum of m-^{3}(4-MeBP·H_2O).

carbonyl oxygen to produce the transient species ^{3}(4-MeBP·H^+). Then, an acid-catalyzed photohydration reaction takes place to produce m-^{3}(4-MeBP·H_2O) and o-^{1}(4-MeBP·H_2O), which partially decays to the ground state of 4-MeBP.

Figure 6a displays the ns-TR^3 spectra obtained for 3-MeBP in a pH 2 CH_3CN/H_2O (1/1) solution after 266 nm excitation and employing a 319.9 nm probe wavelength. The first species observed (marked with a black dashed line) is assigned to ^{3}(3-MeBP), due to the great resemblance of its Raman spectrum to that obtained in CH_3CN (Figure 3S, Supporting Information). Then, a new species emerges with a characteristic Raman band at 1510 cm^{-1} (marked with magenta dashed lines) from 50 to 700 ns. In addition, another species with a characteristic Raman band at 1480 cm^{-1} coexists in the time region from 100 to 300 ns (marked with a blue dashed line). As the delay time increases further, a relatively long-lived species appears with a characteristic Raman band at 1620 cm^{-1}, which is similar to the Raman spectrum of the o-^{1}(4-MeBP·H_2O) species. This assignment is supported by the close similarity of the experimental spectrum with the calculated Raman spectrum of ^{1}(3-MeBP·H_2O) (Figure 13S, Supporting Information). Because m-^{3}(4-MeBP·H_2O) was detected after ^{3}(4-MeBP) decayed, the predicted Raman spectrum of m-^{3}(3-MeBP·H_2O) was also calculated (Figure 7a). Comparison of parts a and b of Figure 7 suggests that the species with a characteristic Raman band at 1510 cm^{-1} (marked with magenta dashed lines) is probably not m-^{3}(3-MeBP·H_2O), since it is missing a Raman signal at 1480 cm^{-1}. An oxygen quenching experiment (Figure 14S, Supporting Information) shows that the Raman band at 1510 cm^{-1} is obviously attenuated via exposure to oxygen purging in comparison to that obtained under an open air environment, suggesting the new species probably has a triplet nature. In a pH 1 aqueous solution (Figure 6b), the new species (marked with a magenta dashed line) is observed upon irradiation and its respective Raman band at 1510 cm^{-1} obviously increases in comparison to that in a pH 2 aqueous solution. A plot of the integrated areas obtained in Figure 6b for the new species using a marker band at 1510 cm^{-1} as a function of time delay is obtained by a one-exponential-term fit, and this result is shown in Figure 15S (Supporting Information). The remarkable differences in the experimental results for 3-MeBP

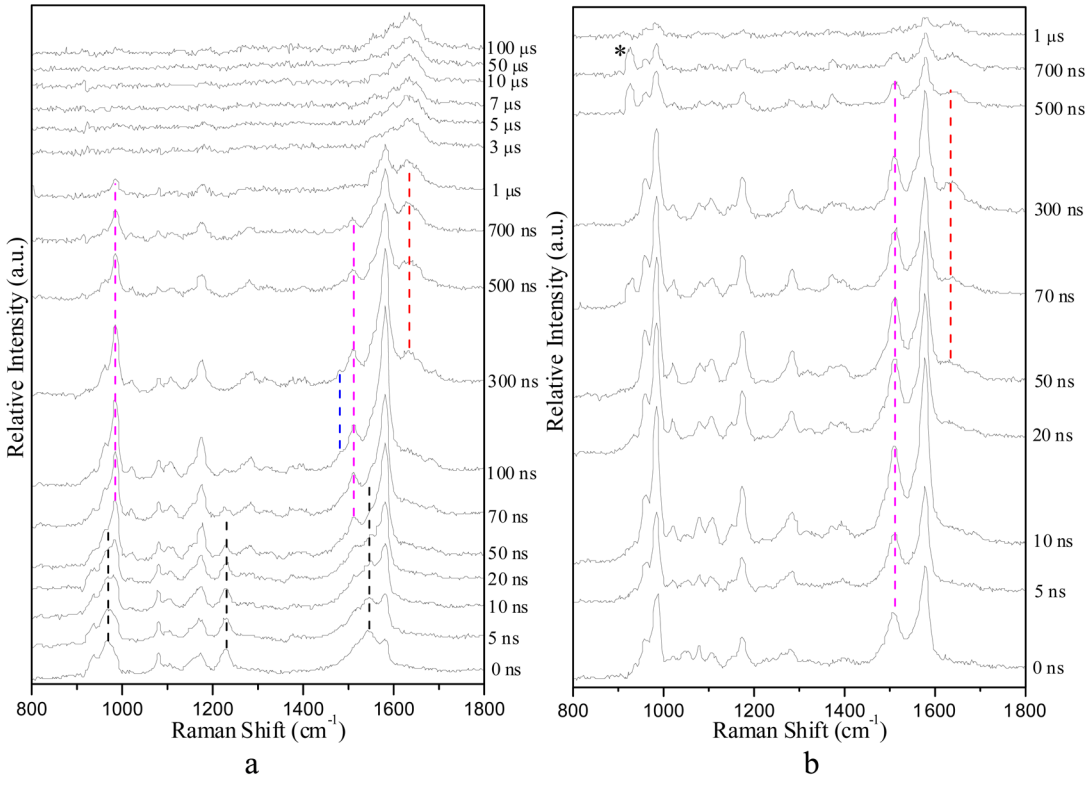

Figure 6. ns-TR^3 spectra of 2.0×10^{-3} M 3-MeBP in CH_3CN/H_2O (1/1) solutions with (a) pH 2 and (b) pH 1 acquired after 266 nm excitation with a probe wavelength of 319.9 nm.

dx.doi.org/10.1021/jo400413t | J. Org. Chem. 2013, 78, 4867−4878

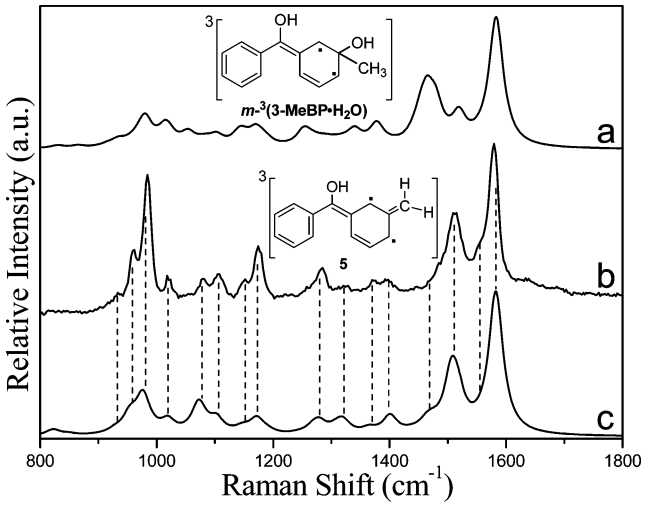

Figure 7. (a) Calculated normal Raman spectrum of m-^{3}(3-MeBP·H_2O). (b) Experimental spectrum obtained at a 20 ns time delay in a pH 1 CH_3CN/H_2O (1/1) solution with 2.0×10^{-3} M of 3-MeBP. (c) Calculated normal Raman spectrum of the intermediate species **5** in Scheme 1.

in acidic aqueous solutions in comparison to those for BP and 4-MeBP suggests that this species (~1510 cm^{-1}) results from an unusual photochemical process rather than the photohydration reaction. Steady-state studies on 3-MeBP by Wan and our previous time-resolved investigations on *m*-BPOH and 2-HEAQ suggest the *m*-methyl activation reaction of 3-MeBP is probably the unusual reaction being observed. The transient species ^{3}(3-MeBP·H^+) observed in fs-TA spectra at later time delays showed noticeable decay in intensity, and the new species observed in the ns-TR^3 spectra was seen upon irradiation and exhibited a noticeable growth in intensity at early time delays. Therefore, the Raman spectrum of the intermediate **5** (which is the species produced from ^{3}(3-MeBP·H^+) in the proposed *m*-methyl activation mechanism in Scheme 1) was simulated (Figure 7c) and compared with the experimental Raman spectrum of the new species seen in the ns-TR^3 spectra (Figure 7b). The excellent agreement in the vibrational frequency patterns for the spectra shown in Figure 7b,c indicates that the new species detected in acidic aqueous solutions (pH <2) of 3-MeBP is the intermediate **5**. This assignment is similar to results of a recent study for *m*-BPOH that detected a new reactive intermediate species associated with *meta* activation of the CH_2OH moiety, which gave rise to a novel and very efficient photoredox reaction with a quantum yield up to 0.6.[2c] The intermediate **5** Raman spectrum profile and structural features observed here have some similarity to the key reactive intermediate observed for the photoredox reaction of *m*-BPOH in acidic aqueous solutions, and this will be discussed later. TD-DFT calculations were done for the intermediate **5** species, and the predicted excited-state energies and oscillator strengths are displayed in Table 1S (Supporting Information). It is predicted that the intermediate **5** has its strongest oscillator strength around 324.9 nm, which is close to the probe wavelength (319.9 nm) used in the ns-TR^3 experiments. This provides further support for the assignment of the new species seen in the ns-TR^3 spectra to the intermediate **5**. It is reasonable to think that the protonated species ^{3}(3-MeBP·H^+) with a positive charge located at the *meta* position is not stable in polar solvents (such as water here) and may give a driving force for deprotonation of the *m*-methyl group by forming the more stable intermediate **5**. After the intermediate **5** is formed, it undergoes an ISC process to form the zwitterionic species **6** (see Scheme 1) on the basis of Wan and co-workers' studies that photolysis of 3-MeBP in D_2O gives rise to a deuterated product[2b] that is more stable in an aqueous solution due to the solvent's high dielectric constant.

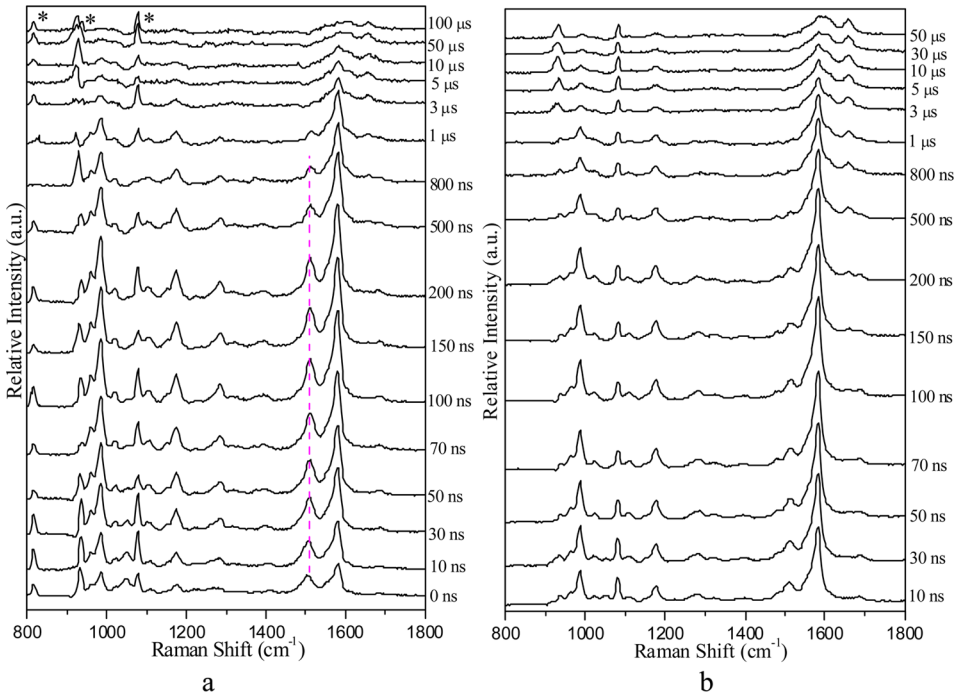

Figure 8. ns-TR^3 spectra of 3-MeBP in pH 0 CH_3CN/H_2O (1/1, v/v) with concentrations of (a) 2.0×10^{-3} M and (b) 5.0×10^{-3} M obtained after 266 nm photolysis and using a 319.9 nm probe wavelength.

dx.doi.org/10.1021/jo400413t | J. Org. Chem. 2013, 78, 4867−4878

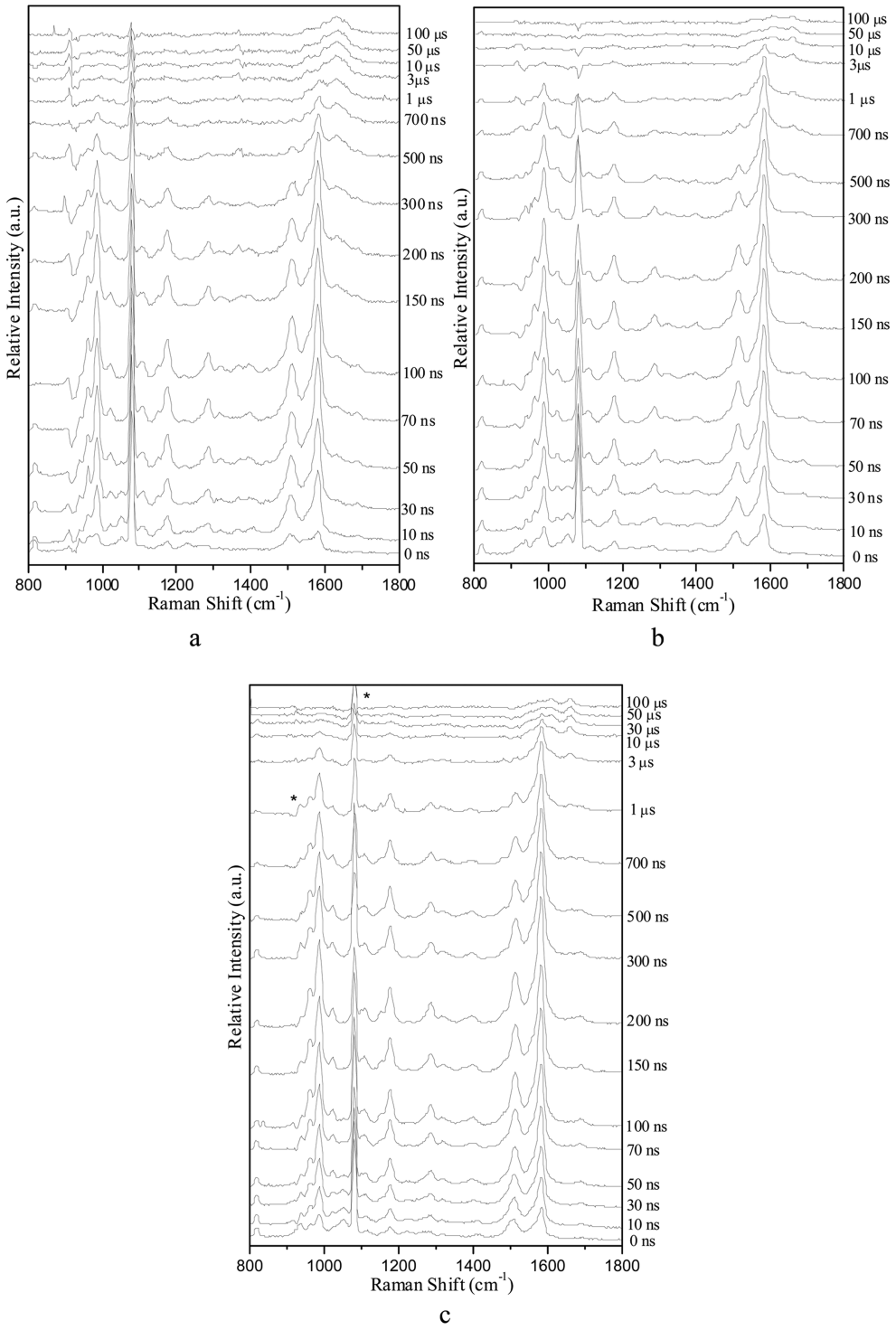

Figure 9. ns-TR^3 spectra of 2.0×10^{-3} M 3-MeBP in CH_3CN/H_2O (v/v) solution at pH 0 with water concentrations of (a) 10%, (b) 30%, and (c) 70% obtained after 266 nm excitation and using a 319.9 nm probe wavelength.

Figure 8a displays the ns-TR^3 spectra acquired for 2.0×10^{-3} M of 3-MeBP in a pH 0 aqueous solution. Because the intermediate **5**, *m*-^{3}(3-MeBP·H_2O), and *o*-^{1}(3-MeBP·H_2O) all contribute to the Raman band at 1580 cm^{-1}, the intensity of the characteristic Raman band for *o*-^{1}(3-MeBP·H_2O) (1630 cm^{-1}, marked with a red dashed line) was monitored as an indicator to measure the efficiency of the photohydration reaction. Inspection of the data shows that the Raman band intensity of *o*-^{1}(3-MeBP·H_2O) decreased as the pH value of the sample solutions varied from 2 to 1 to 0. In an aqueous solution at pH 0, almost no discernible Raman signal of *o*-^{1}(3-MeBP·H_2O) was detected. It appears that the *m*-methyl activation of 3-MeBP is acid-catalyzed and reaches its maximum efficiency at pH 0 under the experimental conditions investigated here. The ns-TR^3 experiments conducted with 5 and 10 mM concentrations (Figure 8b) of 3-MeBP in pH 0 aqueous solutions reveal that with substrate concentrations up to 5 mM no transient species **5** is detected. Nevertheless, the

dx.doi.org/10.1021/jo400413t | J. Org. Chem. 2013, 78, 4867−4878

observed Raman spectra display characteristic spectra similar to those for the ketyl radical species obtained in IPA, which is probably generated from an intermolecular hydrogen abstraction reaction between the substrate molecules under high concentration conditions. This result is in agreement with results from a previous study that showed photolysis with high substrate concentrations gives increasing yields of side reactions due to intermolecular hydrogen abstraction and decreasing the concentration of 3-MeBP does not influence the yield of the deuterated product.[2] The ns-TR[3] experiments with different water concentration solutions at pH 0 (see Figure 9; the decay time of the species **5** is given in Figure 16S (Supporting Information)) indicate that *m*-methyl activation is promoted as the water concentration increases. Furthermore, since it has been elucidated that the $\pi\pi^*$ configuration is preferred in rich water concentration solutions,[8−17] the *m*-methyl activation most likely proceeds via a species with some $\pi\pi^*$ triplet character.

The observation of the reactive intermediate **5** reveals that an unusual methyl activation reaction takes place for 3-MeBP in acidic aqueous solutions (pH <2). Comparison of the experimental results conducted in aqueous solutions with different acid concentrations indicates that this reaction is acid-catalyzed with a maximum efficiency at pH 0. The study on the water concentration effect shows that *m*-methyl activation is water-assisted and the intermediate **5** has a $\pi\pi^*$ configuration. However, only the photohydration is detected for the *para* counterpart, suggesting that the methyl activation is a *meta* effect of some kind.

B. DFT Calculations. DFT calculations for 3-MeBP were performed first in a water cluster system to explore whether *m*-methyl activation can plausibly occur in neutral aqueous solutions. The optimized structures of the reaction complexes (RC_n), transient states (TS_n), and product complexes (PC_n) (in which *n* represents the number of the reaction step in the reaction pathway) obtained from (U)B3LYP/6-311G** calculations for the reaction of ^{3}(3-MeBP) with two water molecules in the system are displayed in Figure 17S (Supporting Information). Figure 10 presents the reaction energy profile for the *meta* activation reaction of ^{3}(3-MeBP) with the assistance of two water molecules. The energy barrier for the protonation process is 14.42 kcal/mol, and that for the deprotonation of the methyl group is 8.28 kcal/mol. Because the DFT calculations tend to underestimate the reaction barrier (an average of 4.4 kcal/mol for a database of 76 barrier heights for B3LYP),[18,19] it is suggested that the protonation process would not be easily accessible in neutral aqueous solutions under experimental conditions. This calculation result is consistent with the experimental observations that no obvious methyl activation reaction was observed for 3-MeBP in a neutral aqueous solution (see Figure 18S, Supporting Information).

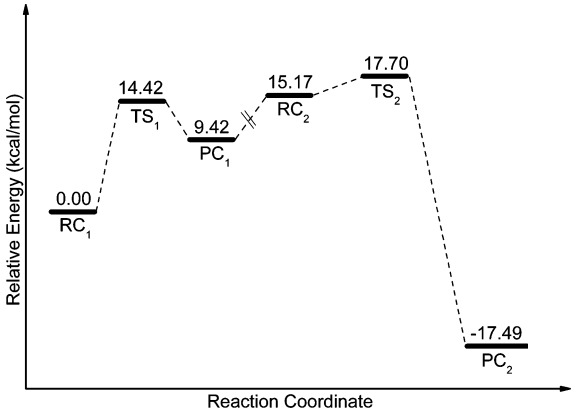

Figure 10. Reaction energy profile obtained from (U)B3LYP/6-311G** calculations for the *m*-methyl activation of ^{3}(3-MeBP) with the assistance of two water molecules.

Since acid is found to be a requisite for *m*-methyl activation from experimental results, we designed some calculations involving an $HClO_4$ molecule (to mimic the acid used in the experiments) in the reaction system. Figure 11 shows the optimized geometries for the RC_n, TS_n and PC_n species obtained from the (U)B3LYP/6-311G** calculations for the reaction of ^{3}(3-MeBP) with a $HClO_4$ molecule. First, the $HClO_4$ molecule provides a pathway for the protonation of the carbonyl oxygen through a connection of the hydrogen bonds. The O−H distance of the $HClO_4$ molecule lengthens from 1.117 Å in TS_1 to 1.809 Å in PC_1, leading to the cleavage of the O−H bond in the $HClO_4$ molecule. At the same time, the interatomic distance between the O atom in the carbonyl group with the H atom in the $HClO_4$ molecule shortens from 1.702 to 1.306 Å, and finally protonation is completed with the formation of bond of the O atom in the carbonyl group with the H atom from the $HClO_4$ molecule formed (O−H bond length of 0.980 Å). Generation of the protonation product PC_1 is consistent with the fs-TA experiment observation of the intermediate species ^{3}(3-MeBP·H$^+$) in acid aqueous solutions. As was discussed earlier, the formation of the protonated species at the carbonyl oxygen undergoes a charge transfer process and the intermediate ^{3}(3-MeBP·H$^+$) observed by the fs-TA experiments has contributions mostly from the intermediate **4** (Scheme 1), where the positive charge is mainly located at the *meta* position of the benzene ring bearing the methyl group. In the second reaction step, the ClO_4 formed from the first reaction step abstracts an H atom in the methyl group by reforming an $HClO_4$ molecule. The C−C bond length between the carbon atom at the *meta* position of the benzene ring and the methyl group decreases from 1.490 Å in RC_2 to have some double bond character 1.405 Å in PC_2. After protonation at the carbonyl oxygen and deprotonation of the methyl group, PC_2 is generated, which is consistent with the detection of intermediate **5** observed in the ns-TR[3] experiments. Figure 12a,b and Figure 19S (Supporting Information) display the reaction energy profiles for the *meta* activation reaction of ^{3}(3-MeBP) with the assistance of $HClO_4$ under vacuum, in H_2O and in CH_3CN, respectively. Activation free energies at 298 K for the protonation and the deprotonation processes under vacuum, in CH_3CN and in H_2O are given in Table 2. Inspection of Table 2 indicates that the introduction of $HClO_4$ results in a small barrier (3.32 kcal/mol) for the protonation of the carbonyl oxygen, followed by a small barrier for deprotonation (3.26 kcal/mol) of the methyl group. This indicates that acid can catalyze the methyl activation reaction. After a water solvent correction, the activation barrier substantially decreases toward a negative result (−0.96 kcal/mol). This result suggests that the protonation of the triplet carbonyl oxygen occurs spontaneously, which is consistent with the fs-TA experimental results. On the other hand, the activation barrier for the deprotonation process is elucidated to be the decisive step. The small activation barrier and the lower energy of the product PC_2 in comparison to those of RC_1 and TS_n reveal that the methyl activation reaction is adiabatic

dx.doi.org/10.1021/jo400413t | J. Org. Chem. 2013, 78, 4867−4878

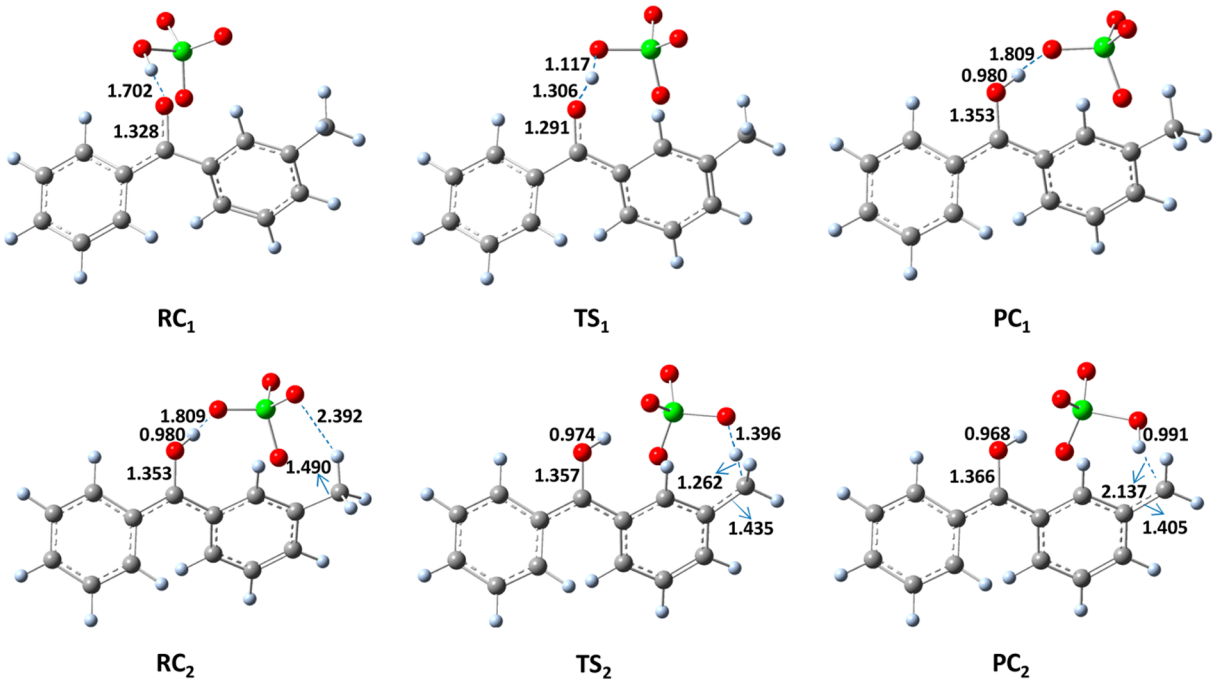

Figure 11. Optimized geometries for RC_n, TS_n, and PC_n obtained from (U)B3LYP/6-311G** calculations for the *meta* activation reaction of (3-MeBP)[3] with $HClO_4$. Selected interatomic distances (in Å) are labeled.

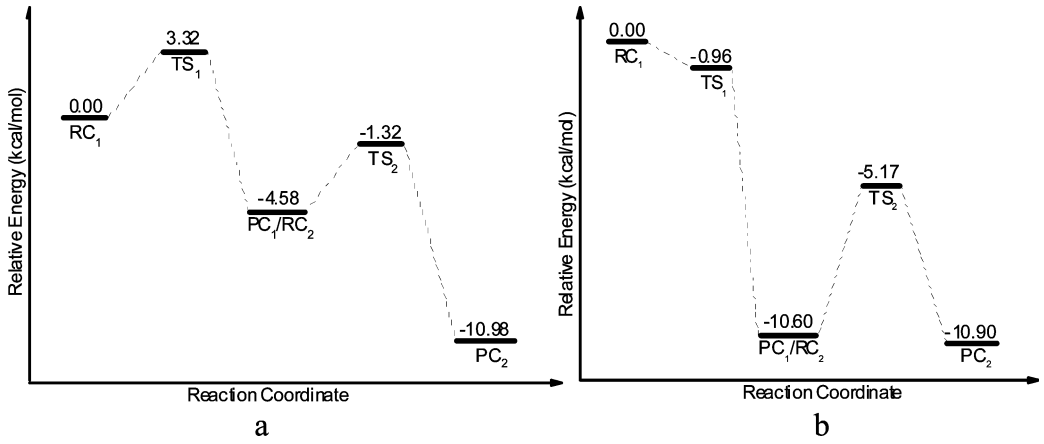

Figure 12. Reaction energy profiles obtained from (U)B3LYP/6-311G** calculations for the *meta* activation reaction of ^{3}(3-MeBP) with the assistance of $HClO_4$ (a) under vacuum and (b) in H_2O are shown.

Table 2. Activation Free Energies (kcal/mol) at 298 K for the Protonation and Deprotonation Processes of ^{3}(3-MeBP) with the Assistance of $HClO_4$ under Vacuum, in CH_3CN (ε = 36.64) and in H_2O (ε = 78.39)

	$\Delta G^{\ddagger}$		
	vacuum	CH_3CN	H_2O
protonation step	3.32	0.37	−0.96
deprotonation step	3.26	4.70	5.43

and favorable both kinetically and thermodynamically. These calculation results are in good agreement with the time-resolved spectroscopy results detailed here and the previous product analysis study reported by Wan and co-workers.[2]

We also studied the character of the molecular orbitals of the key intermediates, which are important for understanding the reactions of the 3-MeBP and 4-MeBP compounds in acidic aqueous solutions. The frontier orbitals for the ^{3}(3-MeBP·H$^+$) and ^{3}(4-MeBP·H$^+$) key intermediates obtained from DFT calculation are respectively shown in Figure 13 and Figure 14. The frontier molecular orbitals comprising the SOMO1 to the SOMO2 contribute to their excited-state transitions. Inspection of Figures 13 and 14 reveals that the SOMO1/SOMO2 orbitals are largely the same for both ^{3}(3-MeBP·H$^+$) and ^{3}(4-MeBP·H$^+$). Since the SOMO1 with π-type symmetry is significantly localized on the phenyl ring not containing the methyl substituent, we turn our attention to the analysis of SOMO2, where the electron mainly resides on the C1 and C3 atoms and the density on the C2 atom is low. For ^{3}(3-MeBP·H$^+$), this positive charge character of the C2 atom can significantly stabilize the carbon anion resulting from the deprotonation of the methyl moiety and thus facilitates the deprotonation process of the C−H bond and is consistent with the experimental observation of the methyl activation reaction for 3-MeBP photochemistry in an acidic aqueous solution. On the other hand, the preferred population of the electron on the

dx.doi.org/10.1021/jo400413t | J. Org. Chem. 2013, 78, 4867−4878

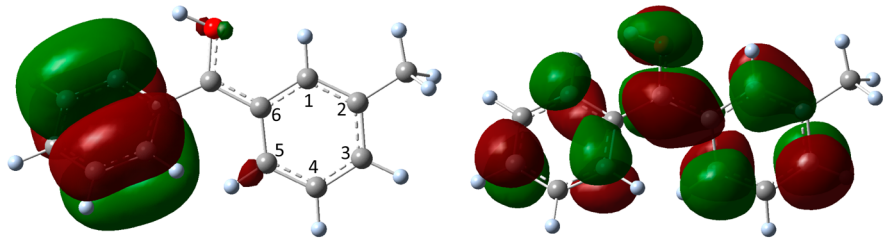

a. SOMO1 b. SOMO2

Figure 13. (a) SOMO1 and (b) SOMO2 frontier orbitals for ^{3}(3-MeBP·H$^+$) obtained from the DFT calculations.

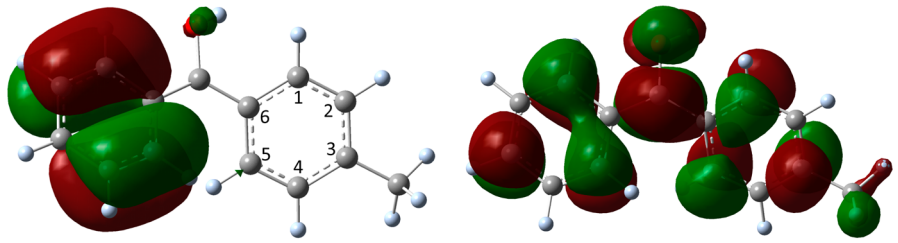

a. SOMO1 b. SOMO2

Figure 14. (a) SOMO1 and (b) SOMO2 frontier orbitals for ^{3}(4-MeBP·H$^+$) obtained from the DFT calculations.

C3 atom in the ^{3}(4-MeBP·H$^+$) intermediate makes the deprotonation process very unfavorable for this *para*-substituted species and helps explain the experimental observation that, even with the generation of the ^{3}(4-MeBP·H$^+$) intermediate, the methyl activation reaction is absent for 4-MeBP.

The Raman spectrum profile and structural features of intermediate **5** observed here are similar to those of the key reactive intermediate involved in the photoredox reaction of *m*-BPOH in acidic aqueous solutions. In contrast, the quantum yield for the photoredox reaction of *m*-BPOH ($\Phi \approx 0.6$) is distinctly higher than that of the *m*-methyl activation for 3-MeBP ($\Phi \approx 0.1$). This indicates that the reactivity of the photoredox reaction for *m*-BPOH is more efficient than the *m*-methyl activation reaction for 3-MeBP, which can be accounted for by the involvement of the electron-donating hydroxyl group in the side chain for *m*-BPOH.

Both the *m*-methyl activation reaction and the photohydration for 3-MeBP take place, via the formation of the species ^{3}(3-MeBP·H$^+$). DFT calculations were also conducted to simulate the insertion of the OH group to the *meta* position of ^{3}(3-MeBP·H$^+$) leading to the photohydration, and these results are shown in Figures 20S and 21S (Supporting Information). The calculated reaction barrier for the insertion of the OH group to the *meta* position of ^{3}(3-MeBP·H$^+$) is comparable to that for the deprotonation step of the *m*-methyl activation reaction in acidic aqueous solutions. These results explain the observed coexistence of the photohydration with the *m*-methyl activation reaction of 3-MeBP in a moderately acidic aqueous solution (pH 2). The nondetection of the photohydration in a pH 0 mixed aqueous solution may result from the limited amount of OH population under such highly acidic conditions.

A product analysis study indicated that a *meta*-substituted fluorinated BP derivative could undergo an aromatic photosubstitution reaction to efficiently form the corresponding *meta*-hydroxy-substituted BP derivative in acidic aqueous solutions but not in neutral aqueous solutions.[1] On the basis of this similarity to the *m*-methyl activation reactions of 3-MeBP and the photoredox reactions of *m*-BPOH, we tentatively propose that this photosubstitution may also occur via an initial protonation of the carbonyl oxygen group. Preliminary DFT calculations (see the results presented in Figure 20S and Figure 21S (Supporting Information)) were performed for the photosubstitution reaction, taking 3-fluorobenzophenone as an example. The DFT results indicate that the photosubstitution reactions can possibly occur through a reaction mechanism similar to those for the photohydration reaction and the *m*-methyl activation reaction, in which there is a protonation of the carbonyl oxygen group. However, further work is needed to more clearly elucidate the actual photosubstitution reactions of *meta*-substituted fluorinated BP derivatives.

■ CONCLUDING REMARKS

The photophysical and photochemical reactions of 3-MeBP and 4-MeBP have been explored by utilizing fs-TA and ns-TR^3 spectroscopy experiments and DFT calculations. 3-MeBP and 4-MeBP were found to exhibit reactions similar to those of BP, *m*-BPOH, and 2-HEAQ in CH_3CN and IPA solvents. In CH_3CN, both 3-MeBP and 4-MeBP undergo efficient ISC to form their respective triplet excited state species, ^{3}(3-MeBP) and ^{3}(4-MeBP). The ^{3}(3-MeBP) and ^{3}(4-MeBP) intermediates were observed to be substantially quenched by a photoreduction reaction in the IPA solvent. In acidic aqueous solutions (pH $\leq$2), the protonated carbonyl oxygen species ^{3}(3-MeBP·H$^+$) and ^{3}(4-MeBP·H$^+$) were observed by fs-TA

dx.doi.org/10.1021/jo400413t | J. Org. Chem. 2013, 78, 4867−4878

spectra. In the case of 4-MeBP, a photohydration reaction and its intermediates m-^{3}(4-MeBP·H_2O) and o-^{1}(4-MeBP·H_2O) were detected, similar to the analogous photohydration reaction previously characterized for BP. In contrast, an unusual m-methyl activation reaction was observed to compete with the photohydration for 3-MeBP and a new intermediate species **5** (see Scheme 1) was observed. In a more strongly acidic aqueous solution (pH 0) the methyl activation reaction becomes the predominant reaction and the photohydration reaction was not detected for 3-MeBP. This unusual methyl activation reaction for 3-MeBP was found to be acid-catalyzed and water-assisted and does not involve diffusional encounters with substrate molecules.

The protonation of the carbonyl oxygen appears to be necessary for the m-methyl activation observed for 3-MeBP. The protonation of the carbonyl oxygen results from its enhanced basicity in the excited state and has been widely studied.[20] The pK_a value for the triplet protonated excited state BP was determined to be -0.4 ± 0.1 by Wirz and co-workers,[1b] and it may be reasonable to estimate a similar value for ^{3}(3-MeBP·H^+). However, deprotonation of the methyl group at the benzene ring under acidic conditions is unexpected and suggests the methyl moiety behaves like a "superacid"[10] in the excited state so that the deprotonation can take place even in a pH 0 aqueous solution. The m-methyl activation reaction examined here has some similarity to other well-known "*meta*-effect" reactions. Although Zimmerman and co-workers examined the *meta* effect as an excited singlet state phenomenon and much of the published reports on *meta*-effect reactions take place via singlet excited states, there are some studies suggesting that *meta*-effect reactions are not restricted only to excited states[21] or to singlet states.[22] The photodecarboxylations for ketoaromatics with the ketone positioned *meta* to the acetic acid functional group show reactivity higher than those with a *para* arrangement, and these reactions may be thought of as an example of some *meta* effect on the photochemistry.[23,24] The m-methyl activation for 3-MeBP, m-BPOH, and 2-HEAQ via triplet excited state intermediates also appear to be interesting cases of *meta*-effect photochemistry.

Our recent time-resolved spectroscopy studies of the photochemistry of *meta*-substituted BP and AQ compounds indicate that the protonation of the carbonyl oxygen opens a new door to new and unusual photochemical reactions such as m-methyl activation and photoredox reactions not seen for the *para*-substituted derivatives. One can expect that these new photochemical reactions for *meta*-substituted aromatic carbonyl compounds in acidic aqueous solutions can be utilized for a variety of applications in the future.

EXPERIMENTAL AND COMPUTATIONAL METHODS

A. Femtosecond Transient Absorption (fs-TA) Experiments. The fs-TA measurements were performed using a regenerative amplified Ti:sapphire laser system and an automated data acquisition system. The probe pulse was obtained by using approximately 5% of the amplified 800 nm output from the laser system to generate a white-light continuum (350−800 nm) in a CaF_2 crystal. The maximum extent of the temporal delay was 3300 ps for the optical stage used in the experiments. The instrument response function was determined to be about 150 fs. At each temporal delay, data were averaged for 2 s. The probe beam was split into two parts before passing through the sample. One portion of the probe beam travels through the sample; the other portion was sent directly to a reference spectrometer that monitored the fluctuations in the probe beam intensity. Fiber optics were coupled to a multichannel spectrometer with a CMOS sensor that had a 1.5 nm intrinsic resolution. For the present experiments, the sample solutions were excited by a 267 nm pump beam (the third harmonic of the fundamental 800 nm from the regenerative amplifier). The 40 mL sample solutions were flowed through a 2 mm path length cuvet throughout the data acquisition. The samples were monitored for degradation by employing UV absorption spectroscopy during the measurements and replaced with fresh samples as needed to avoid noticeable sample degradation effects on the data collected. The data were stored as three-dimensional wavelength−time−absorbance matrices that were exported for use with a fitting software. The sample solutions for the fs-TA experiments were prepared to have an absorbance of 1 at 267 nm so as to have the same number of photons being absorbed for the same irradiating conditions in each case.[25]

B. Nanosecond Time-Resolved Resonance Raman (ns-TR^3) Experiments. The ns-TR^3 experiments were performed using an experimental apparatus and methods described previously in our laboratory,[26] and only a brief account is given here. The 266 nm pump wavelength supplied by the fourth harmonic of a Nd:YAG nanosecond pulsed laser and the 319.9 nm probe wavelength supplied by the third anti-Stokes hydrogen Raman-shifted laser line from the second harmonic of a second Nd:YAG laser were used in the ns-TR^3 experiments. The pump pulse excited the sample to initiate the photochemical reactions, and the probe pulse interrogated the sample and the intermediate species produced by the pump pulse. The laser beams were lightly focused and aligned so that they were overlapped onto a flowing liquid stream of sample. The diameter of the pump beam was adjusted to be slightly larger than that of the probe beam at the overlapping volume in the liquid jet in order to minimize the ground state normal Raman signal. A pulse delay generator was used to electronically control the time delay between the pump and probe laser beams from the two different Nd:YAG lasers operated at a repetition rate of 10 Hz. The Raman scattered light was acquired using a backscattering geometry and then detected by a liquid-nitrogen-cooled charge-coupled device (CCD) detector. The TR^3 signal was acquired for 10 s by the CCD before being read out to an interfaced PC computer, and 10 scans of the signal were accumulated to produce a resonance Raman spectrum. The ns-TR^3 spectra presented in this report were obtained from subtraction of an appropriately scaled probe-before-pump spectrum from the corresponding pump−probe resonance Raman spectrum to remove nontransient bands. The Raman bands of acetonitrile (CH_3CN) were employed to calibrate the Raman shifts of the Raman spectra with an estimated accuracy of 5 cm^{-1}.

C. Density Functional Theory (DFT) Calculations. DFT calculations employing the (U)B3LYP method with a 6-311G** basis set were done to determine the optimized geometries and vibrational wavenumbers for the species that were considered to be potential intermediates. The Raman spectra were obtained using the default G03 method that utilized the determination of the Raman intensities from the transition polarizabilities calculated by a numerical differentiation and with an assumed zero excitation frequency (e.g., the Placzek approximation). A Lorentzian function with a 15 cm^{-1} bandwidth was used for the Raman vibrational frequencies and the relative intensities to obtain the computed Raman spectra that were compared to the experimental TR^3 spectra. A frequency scaling factor of 0.974 was used in the comparison of the calculated results with the experimental spectra. No imaginary frequency modes were observed at the stationary states of the optimized structures shown here, and only one imaginary frequency was observed for the saddle point transition state structures. The reactions examined here have been explored by optimizing the structures of the reactant (RC), transition states (TS), and product complexes (PC). Transition states were located using the Berny algorithm. Frequency calculations at the same level of theory have also been performed to identify all of the stationary points as minima for transition states (one imaginary frequency). The particular nature of the transition states has been determined by analyzing the motion described by the eigenvector associated with the imaginary

dx.doi.org/10.1021/jo400413t | J. Org. Chem. 2013, 78, 4867−4878

frequency. Intrinsic reaction coordinates (IRC)[27] were calculated for the transition states to confirm that the relevant structures connect the two relevant minima. The calculations presented in this study were done using the Gaussian 03 program[28] suite installed on the High Performance Computing cluster at the Computer Centre in The University of Hong Kong.

■ ASSOCIATED CONTENT

Supporting Information

Figures and tables giving a UV−vis absorption spectrum, fs-TA spectra, and ns-TR^3 spectra for the reported species, optimized geometries of the RC, TS, and PC, the reaction energy profile obtained from the (U)B3LYP/6-311G** calculations and the excited state energies and oscillator strengths from TD-DFT (UB3LYP/6-311G**) calculations for the transient species, and Cartesian coordinates, total energies, and vibrational zero-point energies for the optimized geometry from the (U)-B3LYP/6-311G** calculations for the compounds and intermediates considered in this paper. This material is available free of charge via the Internet at http://pubs.acs.org.

■ AUTHOR INFORMATION

Corresponding Author

*E-mail for D.L.P.: phillips@hku.hk.

Notes

The authors declare no competing financial interest.

■ ACKNOWLEDGMENTS

The research was supported by grants from the Research Grants Council of Hong Kong (HKU 7048/11P) to D.L.P., and partial support from the Areas of Excellence Scheme (AoE/P-03/08) and the Special Equipment Grant (SEG HKU/07) is also gratefully acknowledged.

■ REFERENCES

(1) (a) Klan, P.; Wirz, J. *Photochemistry of Organic Compounds: From Concepts to Practice*; Wiley: Hoboken, NJ, 2009; Online ISBN: 9781444300017. (b) Ramseier, M.; Senn, P.; Wirz, J. *J. Phys. Chem. A* **2003**, *107*, 3305−3315.

(2) (a) Lukeman, M.; Xu, M.; Wan, P. *Chem. Commun.* **2002**, *2*, 136−137. (b) Huck, L. A.; Wan, P. *Org. Lett.* **2004**, *6*, 1797−1799. (c) Devin, M.; Lukeman, M.; Dan, L.; Wan, P. *Org. Lett.* **2005**, *7*, 3387−3389. (d) Basarić, N.; Mitchell, D.; Wan, P. *Can. J. Chem.* **2007**, *85*, 561−571. (e) Hou, Y.; Wan, P. *Photochem. Photobiol. Sci.* **2008**, *7*, 588−596. (f) Hou, Y.; Huck, L. A.; Wan, P. *Photochem. Photobiol. Sci.* **2009**, *8*, 1408−1451.

(3) (a) Zimmerman, H. E. *J. Am. Chem. Soc.* **1995**, *117*, 8988−8991. (b) Zimmerman, H. E. *J. Phys. Chem. A* **1998**, *102*, 5616−5621.

(4) Ma, J.; Li, M.-D.; Phillips, D. L.; Wan, P. *J. Org. Chem.* **2011**, *76*, 3710−3719.

(5) Ma, J.; Su, T.; Li, M.-D.; Du, W.; Huang, J.; Guan, X.; Phillips, D. L. *J. Am. Chem. Soc.* **2012**, *134*, 14858−14868.

(6) O'Boyle, N. M.; Tenderholt, A. L.; Langner, K. M. *J. Comput. Chem.* **2008**, *29*, 839−845.

(7) Du, Y.; Xue, J.; Li, M.-D.; Phillips, D. L. *J. Phys. Chem. A* **2009**, *113*, 3344−3352.

(8) (a) Bhasikuttan, A. C.; Singh, A. K.; Palit, D. K.; Sapre, A. V.; Mittal, J. P. *J. Phys. Chem. A* **1998**, *102*, 3470−3480. (b) Singh, A. K.; Bhasikuttan, A. C.; Palit, D. K.; Mittal, J. P. *J. Phys. Chem. A* **2000**, *104*, 7002−7009.

(9) (a) Mitsui, M.; Ohshima, Y. *J. Phys. Chem. A* **2000**, *104*, 8638−8648. (b) Mitsui, M.; Ohshima, Y.; Ishiuchi, S.-i.; Sakai, M.; Fujii, M. *J. Phys. Chem. A* **2000**, *104*, 8649−8659. (c) Mitsui, M.; Ohshima, Y.; Kajimoto, O. *J. Phys. Chem. A* **2000**, *104*, 8660−8670.

(10) (a) Morlet-Savary, F.; Ley, C.; Jacques, P.; Wieder, F.; Fouassier, J. P. *J. Photochem. Photobiol. A: Chem.* **1999**, *126*, 7−14. (b) Ley, C.; Morlet-Savary, F.; Jacques, P.; Fouassier, J. P. *Chem. Phys.* **2000**, *255*, 335−346.

(11) Cavaleri, J. J.; Prater, K.; Bowman, R. M. *Chem. Phys. Lett.* **1996**, *259*, 495−502.

(12) van der Burgt, M. J.; Jansen, L. M. G.; Huizer, A. H.; Varma, C. A. G. O. *Chem. Phys.* **1995**, *201*, 525−538.

(13) Hamanoue, K.; Nakayama, T.; Yamaguchi, T.; Ushida, K. *J. Phys. Chem.* **1989**, *93*, 3814−3818.

(14) (a) Scaiano, J. C. *J. Am. Chem. Soc.* **1980**, *102*, 7747−7753. (b) Cosa, G.; Purohit, S.; Scaiano, J. C.; Bosca, F.; Miranda, M. A. *Photochem. Photobiol.* **2002**, *75*, 193−200.

(15) Dalton, J. C.; Montgomery, F. C. *J. Am. Chem. Soc.* **1974**, *96*, 6230−6232.

(16) Rusakowicz, R.; Byers, G. W.; Leermakers, P. A. *J. Am. Chem. Soc.* **1971**, *93*, 3263−3266.

(17) Palit, D. K. *Res. Chem. Intermed.* **2005**, *31*, 205−225.

(18) Zhao, Y.; González-García, N.; Truhlar, D. G. *J. Phys. Chem. A* **2005**, *109*, 2012−2018.

(19) Zhao, Y.; Truhlar, D. G. *Acc. Chem. Res.* **2008**, *41*, 157−167.

(20) Tolbert, L. M.; Solntsev, K. M. *Acc. Chem. Res.* **2002**, *35*, 19−27.

(21) Foti, M. C.; Daquino, C.; DiLabio, G. A.; Ingold, K. U. *J. Org. Chem.* **2008**, *73*, 2408−2411.

(22) Dichiarante, V.; Dondi, D.; Protti, S.; Fagnoni, M.; Albini, A. *J. Am. Chem. Soc.* **2007**, *129*, 5605−5611; **2007**, *129*, 11662 (correction).

(23) Xu, M.; Wan, P. *Chem. Commun.* **2000**, 2147−2148.

(24) Blake, J. A.; Gagnon, E.; Lukeman, M.; Scaiano, J. C. *Org. Lett.* **2006**, *8*, 1057−1060.

(25) Kochevar, I. E.; Redmond, R. W. In *Methods in Enzymology*, Abelson, J. N., Simon, M. I., Eds.; Academic Press: New York, 2000; Vol. *319*, p 20.

(26) Ma, C.; Kwok, W. M.; Chan, W. S.; Du, Y.; Kan, W. J. T.; Toy, P. H.; Phillips, D. L. *J. Am. Chem. Soc.* **2006**, *128*, 2558−2570.

(27) Cancès, E.; Mennucci, B.; Tomasi, J. *J. Chem. Phys.* **1997**, *107*, 3032−3041.

(28) Frisch, M. J.; Trucks, G. W.; Schlegel, H. B.; Scuseria, G. E.; Robb, M. A.; Cheeseman, J. R.; Scalmani, G.; Barone, V.; Mennucci, B.; Petersson, G. A.; Nakatsuji, H.; Caricato, M.; Li, X.; Hratchian, H. P.; Izmaylov, A. F.; Bloino, J.; Zheng, G.; Sonnenberg, J. L.; Hada, M.; Ehara, M.; Toyota, K.; Fukuda, R.; Hasegawa, J.; Ishida, M.; Nakajima, T.; Honda, Y.; Kitao, O.; Nakai, H.; Vreven, T.; Montgomery, J. A., Jr.; Peralta, J. E.; Ogliaro, F.; Bearpark, M.; Heyd, J. J.; Brothers, E.; Kudin, K. N.; Staroverov, V. N.; Kobayashi, R.; Normand, J.; Raghavachari, K.; Rendell, A.; Burant, J. C.; Iyengar, S. S.; Tomasi, J.; Cossi, M.; Rega, N.; Millam, J. M.; Klene, M.; Knox, J. E.; Cross, J. B.; Bakken, V.; Adamo, C.; Jaramillo, J.; Gomperts, R.; Stratmann, R. E.; Yazyev, O.; Austin, A. J.; Cammi, R.; Pomelli, C.; Ochterski, J. W.; Martin, R. L.; Morokuma, K.; Zakrzewski, V. G.; Voth, G. A.; Salvador, P.; Dannenberg, J. J.; Dapprich, S.; Daniels, A. D.; Farkas, Ö.; Foresman, J. B.; Ortiz, J. V.; Cioslowski, J.; Fox, D. J. *Gaussian 03*; Gaussian, Inc., Wallingford, CT, 2004.